Electromagnetic transitions of $(b\bar{c})$ bound system

Sonali Patnaik,[1] P. C. Dash,[1] Susmita Kar,[2,*] and N. Barik[3]

[1]Department of Physics, Siksha 'O' Anusandhan Deemed to be University, Bhubaneswar-751030, India
[2]Department of Physics, North Orissa University, Baripada-757003, India
[3]Department of Physics, Utkal University, Bhubaneswar-751004, India

(Received 1 February 2018; published 29 March 2018)

We study the electromagnetic transitions $B_c^*(ns) \to B_c(ns)e^+e^-$, $B_c^*(ns) \to B_c(n's)e^+e^-$, and $B_c(ns) \to B_c^*(n's)e^+e^-$ in the relativistic independent quark (RIQ) model based on a flavor-independent potential in the scalar-vector harmonic form. The transition form factors for energetically possible transitions involving B_c and B_c^* mesons in ground as well as orbitally excited states are predicted in their respective kinematic range. Our predictions on decay width for the allowed and hindered transitions are found to be compatible with those of the model calculations based on the Bethe-Salpeter approach. Predictions in this sector would not only provide more information about members of the B_c family, including mass splitting between vector mesons and corresponding pseudoscalar counterparts, but also give hints about the experimental determination of unknown masses of other excited B_c mesons and the ground state B_c^* meson, which is expected at LHCb and Z^0 factory in the near future.

DOI: 10.1103/PhysRevD.97.056025

I. INTRODUCTION

Ever since its discovery at Fermilab by the CDF Collaboration [1], the B_c meson has been attracting a great deal of attention both theoretically and experimentally. The mesons in the $b\bar{c}$ (B_c) family lie intermediate in mass and size between charmonium $(c\bar{c})$ and bottomonium $(b\bar{b})$ family, where the heavy quark interactions are believed to be understood rather well. The B_c meson with explicitly two heavy quarks has not yet been thoroughly studied because of insufficient data available in this sector. Even though the ground state B_c of $J^P = 0^-$ was found several years ago, its partner B_c^* of $J^P = 1^-$ has not yet been seen. Earlier attempts [2–4] to observe B_c at the e^+e^- collider could not succeed since the luminosity and collision energy, as that of LEP-I and II, could result in only small statistics for B_c events [5–7]. With the observation of B_c at hadron colliders, particularly TEVATRON [8,9], a detailed study of B_c family members is expected at the LHC, where the available energy and luminosity are much higher than at TEVATRON and should result in a thousand times more B_c events. The lifetime of B_c has been measured [10–13] using decay channels: $B_c^\pm \to J/\psi e^\pm \bar{\nu}_e$ and $B_c^\pm \to J/\psi\pi^\pm$. At LHCb, a more precise B_c lifetime is obtained [14] using the decay mode $B_c \to J/\psi\mu\nu_\mu X$, where X denotes any possible additional particle in the final state. Recently, the ATLAS Collaboration at LHC has detected the excited B_c state [15] through the channel $B_c^\pm(2s) \to B_c^\pm(1s)\pi^+\pi^-$ by using 4.9 fb^{-1} of 7 TeV and 19.2 fb^{-1} of 8 TeV pp collision data, yielding the $B_c(2s)$ meson mass $\sim 6842 \pm 4 \pm 5$ MeV. Here, the problem encountered is that the messy QCD background of the hadron colliders contaminating the environment makes precise measurement difficult and, therefore, observation of excited B_c states and the B_c^* ground state is almost impossible at the LHC. In this respect, the proposed Z^0 factory offers a conducive environment for measurement. The Z^0 factory, an e^+ e^- collider, running at the Z^0 boson pole with sufficiently higher luminosity and offering relatively cleaner background is supposed to enhance the event-accumulation rate so that other excited B_c states and possibly the B_c^* ground state are likely to be observed in the near future.

Unlike heavy quarkonia, the B_c meson with explicitly two heavy quark constituents does not annihilate to photons or gluons. The ground state B_c meson can, therefore, decay weakly through $b \to cW^-$; $\bar{c} \to \bar{s}W^-$ or decay radiatively through $b \to b\gamma$; $\bar{c} \to \bar{c}\gamma$ at the quark level. A possible measurement of radially excited states of B_c via $B_c(ns) \to B_c\pi\pi$ at LHC and the Z^0 factory is discussed in Ref. [16]. However, the splitting between $B_c(1s)$ and its nearest member $B_c^*(1s)$ due to possible spin-spin interaction estimated in the range $30 \le \Delta m \le 50$ MeV [17] forbids the process $B_c^* \to B_c + \pi^0(\eta, \eta')$ by energy-momentum conservation. Therefore, the dominant decay modes in this sector are the magnetic dipole transitions of the type

*skar09.sk@gmail.com

$B_c^*(ns) \to B_c(ns)\gamma$ and $B_c(ns) \to B_c^*(n's)\gamma$ with $n > n'$. Another decay mode of interest is $B_c^*(ns) \to B_c(ns)e^+e^-$ which is also governed by the electromagnetic process, where the emitted photon is an off-shell virtual one. Compared to radiative decays emitting real photons, the rate of these decay processes is thought to be highly suppressed due to a tight three body phase space and an extra electromagnetic vertex. These processes are more interesting theoretically because the lepton pair (e^+, e^-) product could be easily caught by the detector as clear signals. Being charged particles, their track can be more easily identified than that of the neutral photon emitted in M1 radiative decays of B_c and B_c^*.

Several theoretical attempts [17–31] including different versions of potential models based on the Bethe-Salpeter (BS) approach, light front quark (LFQ) model, QCD sum rules and Lattice QCD (LQCD) etc. have predicted the B_c-spectrum, its mass and decay widths. We have analyzed various M1 transitions of the type $V \to P\gamma$ and $P \to V\gamma$ in the light and heavy flavor sector within and beyond static approximation [32] in the framework of relativistic independent quark (RIQ) model. We have also studied the q^2-dependence of relevant transition form factors and predicted decay widths for radiative decays of heavy mesons in the charm and bottom flavor sector [33] and recently predicted the magnetic dipole transitions of the ground and excited B_c and B_c^* mesons [34] in good comparison with other model predictions. The applicability of RIQ model has already been tested in describing wide ranging hadronic phenomena including the static properties of hadrons [35] and various decays such as radiative, weak radiative and rare radiative [32,36]: leptonic and weak leptonic [37,38] radiative leptonic [39]; semileptonic [40], and nonleptonic [41,42] decays of mesons in the light and heavy flavor sector. KE Hong Wei *et al.* [17] in their analysis of magnetic dipole transitions predicted $B_c^*(ns) \to B_c(ns)e^+e^-$ and $B_c(ns) \to B_c^*(n's)e^+e^-$ with $n > n'$. We would like to extend the applicability of RIQ model to describe such decay modes involving B_c and B_c^* mesons in their ground and excited states. Such a study would be helpful in extracting more information about members of B_c family, determining mass splitting and predicting the decays widths.

The paper is organized as follows: In Sec. II, we give a brief account of RIQ model and describes model expression for the transition form factor and decay width. In Sec. III, we provide our numerical results and discussion. Section IV encompasses our summary and conclusion.

II. TRANSITION MATRIX ELEMENT, TRANSITION FORM FACTOR AND DECAY WIDTH IN RIQ MODEL

The RIQ model framework has been discussed in earlier applications of the model to a wide range of hadronic phenomena [32–41]. For the sake of completeness we provide here a brief description of the model framework and model expressions for constituent quark orbitals along with corresponding momentum probability amplitudes in the Appendix. In a field-theoretic description of any decay process, which in fact occurs physically in the momentum eigenstate of participating mesons, a meson state such as $|B_c(\vec{P}, S_V)\rangle$ is considered at definite momentum $\vec{P}$ and spin state S_V in terms of appropriate wave packet [32–34,36–41] as:

$$|B_c(\vec{P}, S_V)\rangle = \hat{\Lambda}_{B_c}(\vec{P}, S_V)|(\vec{p}_b, \lambda_b); (\vec{p}_c, \lambda_c)\rangle \tag{1}$$

where, $|(\vec{p}_b, \lambda_b); (\vec{p}_c, \lambda_c)\rangle = \hat{b}_b^\dagger(\vec{p}_b, \lambda_b)\hat{\bar{b}}_c^\dagger(\vec{p}_c, \lambda_c)|0\rangle$ is a Fockspace representation of the unbound quark b and antiquark $\bar{c}$ in a color-singlet configuration with their respective momentum and spin as $(\vec{p}_b, \lambda_b)$ and $(\vec{p}_c, \lambda_c)$. Here $\hat{b}_b^\dagger(\vec{p}_b, \lambda_b)$ and $\hat{\bar{b}}_c^\dagger(\vec{p}_c, \lambda_c)$ are, respectively, the quark and antiquark creation operators. $\hat{\Lambda}_{B_c}(\vec{P}, S_V)$ represents a baglike integral operator taken in the form

$$\hat{\Lambda}_{B_c}(\vec{P}, S_V) = \frac{\sqrt{3}}{\sqrt{N_{B_c}(\vec{P})}} \sum_{\lambda_b, \lambda_{\bar{c}}} \zeta_{b,\bar{c}}^{B_c}(\lambda_b, \lambda_{\bar{c}}) \times \int d^3\vec{p}_b d^3\vec{p}_{\bar{c}} \delta^{(3)}(\vec{p}_b + \vec{p}_{\bar{c}} - \vec{P}) \mathcal{G}_{B_c}(\vec{p}_b, \vec{p}_{\bar{c}}). \tag{2}$$

Here $\sqrt{3}$ is the effective color factor, $\zeta_{b,\bar{c}}^{B_c}(\lambda_b, \lambda_{\bar{c}})$ stands for appropriate SU(6)-spin flavor coefficients for the meson. $N(\vec{P})$ is the meson-state normalization which can be realized from $\langle B_c(\vec{P})|B_c(\vec{P}')\rangle = \delta^{(3)}(\vec{P} - \vec{P}')$ in an integral form

$$N(\vec{P}) = \int d^3\vec{p}_b |\mathcal{G}_{B_c}(\vec{p}_b, \vec{P} - \vec{p}_b)|^2 \tag{3}$$

Finally $\mathcal{G}_{B_c}(\vec{p}_b, \vec{P} - \vec{p}_b)$ is the effective momentum profile function for the quark-antiquark pair which in terms of individual momentum probability amplitudes: $G_b(\vec{p}_b)$ and $\tilde{G}_c(\vec{p}_c)$ for quark b and antiquark $\bar{c}$, respectively, is considered in the form

$$\mathcal{G}_{B_c}(\vec{p}_b, \vec{p}_{\bar{c}}) = \sqrt{G_b(\vec{p}_b)\tilde{G}_{\bar{c}}(\vec{p}_{\bar{c}})} \tag{4}$$

in a straightforward extension of the ansatz of Margolis and Mendel in their bag model analysis [43].

In the wave packet representation of meson bound state $|B_c(\vec{P}, S_V)\rangle$, the bound state character is thought to be embedded here in $\mathcal{G}_{B_c}(\vec{p}_b, \vec{p}_{\bar{c}})$. Any residual internal dynamics responsible for decay process such as $B_c^* \to B_c e^+e^-$ can therefore be analyzed at the level of otherwise free quark and antiquark using appropriate Feynman diagrams. Total contributions from Feynman diagram

provides the constituent level S-matrix element $S_{fi}^{b\bar{c}}$ which when operated by the operator $\hat{\Lambda}_{B_c}(\vec{P}, S_V)$ gives the meson-level effective S-matrix element $S_{fi}^{B_c}$ as

$$S_{fi}^{B_c} = \hat{\Lambda}_{B_c}(\vec{P}, S_V) S_{fi}^{b\bar{c}} \tag{5}$$

The hadronic matrix element for $B_c^* \to B_c e^+ e^-$ finds a covariant expansion in terms of transition form factor $F_{B_c^* B_c}(q^2)$ as

$$\begin{aligned}&\langle B_c(k)|J_\mu^{em}|B_c^*(P,h)\rangle \\ &\quad = ie\epsilon_{\mu\nu\rho\sigma}\epsilon^\nu(P,h)(P+k)^\rho(P-k)^\sigma F_{B_c^* B_c}(q^2)\end{aligned} \tag{6}$$

where, $q = (P-k) = k_1 + k_2$ is the four-momentum transfer, k, k_1, k_2 are the four-momentum of B_c, electron and positron, respectively, and $\epsilon_\nu(P,h)$ is the polarization vector of B_c^* with four-momentum P and helicity h. For transition $B_c^* \to B_c e^+ e^-$, the kinematic range of q^2 is $(2m_e)^2 \le q^2 \le (m_{B_c^*} - m_{B_c})^2$. The q^2 dependence of the form factor can be studied using the expression for $F_{B_c^* B_c}(q^2)$ obtainable in the RIQ model.

The decay process $B_c^* \to B_c e^+ e^-$ as depicted in Figs. 1(a) and 1(b) is thought to be predominantly a double-vertex electromagnetic process governed by photon emission at the photon-hadron vertex from independently confined quark b as well as antiquark $\bar{c}$ in the meson bound state $|B_c^*(\vec{P}, S_V)\rangle$. The emitted photon is an off-shell virtual one which ultimately leptonizes into pair of leptons (e^-, e^+). The S-matrix element for the process in configuration space is written as:

$$\begin{aligned}S_{fi} &= \langle B_c(k) e^+(k_1,\delta_1) e^-(k_2,\delta_2)|(-ie)^2 \\ &\quad \times \int d^4x_1 d^4x_2 \bar{\psi}_{e^-}^{(-)}(x_2)\gamma^\mu \psi_{e^+}^{(-)}(x_2)\mathcal{D}_{\mu\nu}(x_2 - x_1) \\ &\quad \times \sum_q e_q \bar{\psi}_q^{(+)}(x_1)\gamma^\nu \psi^{(+)}(x_1)|B_c^*(\vec{P}, S_V)\rangle\end{aligned} \tag{7}$$

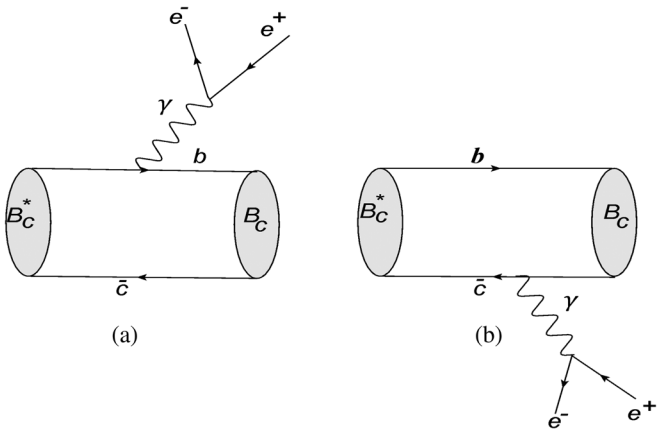

FIG. 1. Lowest-order Feynman diagram contributing electromagnetic transition.

where $\mathcal{D}_{\mu\nu}(x_2 - x_1)$ is photon propagator. Now using usual expression for photon propagator, quark and lepton field expansion and then simplifying hadronic and leptonic part separately by adopting the vacuum insertion technique, S_{fi} in the B_c^* rest frame is obtained in the standard form as

$$\begin{aligned}S_{fi} &= (2\pi)^4 \delta^{(4)}(k + k_1 + k_2 - \hat{O} M_{B_c^*}) \\ &\quad \times \frac{(-i\mathcal{M}_{fi})}{\sqrt{(2\pi)^3 2M_{B_c^*}}} \prod_f \frac{1}{\sqrt{(2\pi)^3 2E_f}}\end{aligned} \tag{8}$$

where, the hadronic part h_μ is found to be

$$\begin{aligned}h_\mu &= \sqrt{2M_{M_c^*} 2E_k} \\ &\quad \times \left[e_b \int d\vec{p}_b \frac{\mathcal{G}_{B_c^*}(\vec{p}_b, -\vec{p}_b)\mathcal{G}_{B_c}(\vec{k} + \vec{p}_b, -\vec{p}_b)}{\sqrt{2E_{p_b} 2E_{p_b+k} N(0) N(\vec{k})}} \mathcal{C}_{\lambda_b \lambda_c \lambda_b'}^{B_c^* B_c} \right. \\ &\quad \left. - e_c \int d\vec{p}_c \frac{\mathcal{G}_{B_c^*}(-\vec{p}_c, \vec{p}_c)\mathcal{G}_{B_c}(-\vec{p}_c, \vec{k} + \vec{p}_c)}{\sqrt{2E_{p_c} 2E_{p_c+k} N(0) N(\vec{k})}} \mathcal{C}_{\lambda_b \lambda_c \lambda_c'}^{B_c^* B_c} \right]\end{aligned} \tag{9}$$

with

$$\begin{aligned}\mathcal{C}_{\lambda_b \lambda_c \lambda_b'}^{B_c^* B_c} &= \sum_{\lambda_b \lambda_c \lambda_b'} \zeta_{b,c}^{B_c^*}(\lambda_b, \lambda_c)\zeta_{b',c}^{B_c}(\lambda_b', \lambda_c) \\ &\quad \times \bar{U}_{b'}(\vec{k} + \vec{p}_b, \lambda_b')\gamma_\mu U_b(\vec{p}_b, \lambda_b) \\ \mathcal{C}_{\lambda_b \lambda_c \lambda_c'}^{B_c^* B_c} &= \sum_{\lambda_b \lambda_c \lambda_b'} \zeta_{b,c}^{B_c^*}(\lambda_b, \lambda_c)\zeta_{b,c'}^{B_c}(\lambda_b, \lambda_c') \\ &\quad \times \bar{V}_c(\vec{p}_c, \lambda_c)\gamma_\mu V_c(\vec{k} + \vec{p}_c, \lambda_c')\end{aligned} \tag{10}$$

and the leptonic part l^μ is

$$l^\mu(k_1, k_2, \delta_1, \delta_2) = \bar{U}_{e^-}(k_2, \delta_2)\gamma^\mu V_{e^+}(k_1, \delta_1) \tag{11}$$

It is worthwhile to mention that the bound state picture of meson considered at a definite momentum and spin state is, of course, not relativistically covariant. This is in fact true with almost all potential models describing meson as a bound state of valence quark and antiquark interacting via some instantaneous potential. Such models, however, are often required to extract the meson level decay amplitudes starting from the Feynman amplitude at constituent level. The problem that one usually encounters here is that although three-momentum conservation has been ensured at the composite level through $\delta^{(3)}(\vec{p}_b + \vec{p}_c - \vec{P})$ in the meson state $|B_c(\vec{P}, S_V)\rangle$, the energy conservation satisfying $E_{B_c} = E_b(\vec{p}_b) + E_c(\vec{p}_c)$ in such definite momentum state is not specified so explicitly. This is indeed a pathological problem common to all such models attempting to describe the decay of hadrons in terms of zeroth-order constituent level dynamics. However, we have shown in our previous

works, in the context of nonleptonic decays of the B and B_c meson [42] and radiative leptonic decays of B_c, B_u, D_s, and D mesons [39], that the energy conservation is ensured in an average sense by the effective momentum distribution profile function used in respective meson states. For example in B_c-meson decays in its rest frame we have realized

$$\langle B_c(0,S_V)|E_b(|\vec{p}_b|^2)+E_c(|-\vec{p}_b|^2)|B_c(0,S_V)\rangle = M_{B_c},$$

where M_{B_c} is the mass of B_c meson. In the wave packet representation of the meson state, the bound state character is thought to be embedded in the dynamical quantity $\mathcal{G}_{B_c}(\vec{p}_b,\vec{p}_c)$. The energy conservation constraint $E_b(\vec{p}_b)+E_c(\vec{p}_c)=M_{B_c}$ assumed in the decaying meson rest frame might lead to spurious kinematic singularities. This has been taken care of in our above mentioned works in the context of radiative leptonic and nonleptonic decays by retaining a definite mass $m_{\bar{c}}$ of the spectator quark $\bar{c}$ while assigning a running mass m_b to the active quark b in the meson state in the form

$$m_b^2(\vec{p}_b) = M_{B_c}^2 - m_c^2 - 2M_{B_c}\sqrt{\vec{p}_b^2+m_c^2}$$

as an outcome of the energy conservation constraint. This has led to an upper bound for the quark momentum $|\vec{p}_b|$ in order to retain $m_b^2(|\vec{p}_b|^2)$ positive definite. In the process we could avoid possible kinematic singularities in the quark level integration. The expectation values of the binding energy of quark and antiquark and that of the sum of their binding energies, have been calculated in the decaying meson rest frame. It is found that the expectation value of binding energy of the quark and antiquark for different meson states are found close to their respective model solutions. We also find that the expectation value of the sum of binding energies of the quark and antiquark in respective meson state are close to their corresponding observed masses [39,42].

This lends credence to our ansatz for energy conservation in our model formalism. This along with momentum conservation via the three-momentum delta function in the meson state ensures energy-momentum conservation in the decay process. Here the invariant decay amplitude is extracted in this model from the Feynman amplitude at constituent level after realizing the required energy-momentum conservation through appropriate four-momentum delta function. Thus our approach in realizing the energy-momentum conservation as pre-requisite for relativistic studies is no doubt a reasonable approach. In the absence of any rigorous field theoretic approach involving bound quark and antiquark, the constituent level description of various decay processes based on such approximation have yielded reasonable predictions in our earlier works [33,34,39,41,42].

Now the timelike component of h_μ in Eq. (9) vanishes identically for each combination of B_c^* spin state with the singlet state of B_c. As a result $\mathcal{M}_{fi}$ is effectively expressed in terms of spacelike parts of the hadronic and leptonic part in the form:

$$\mathcal{M}_{fi} = e^2 h_i l^i(k_1,k_2,\delta_1,\delta_2)/(k_1+k_2)^2 \tag{12}$$

Using usual spin algebra, the non vanishing spacelike hadronic part h_i is obtained as

$$h_i = (e_b I_b + e_c I_c)(\vec{\epsilon}\times\vec{k})_i \tag{13}$$

with

$$I_b = \sqrt{2M_{B_c^*}2E_k}\int d\vec{p}_b \frac{\mathcal{G}_{B_c^*}(\vec{p}_b,-\vec{p}_b)\mathcal{G}_{B_c}(\vec{p}_b+\vec{k},-\vec{p}_b)}{\sqrt{2E_{p_b}2E_{p_b+k}\bar{N}_{B_c^*}(0)\bar{N}_{B_c}(\vec{k})}}\sqrt{\frac{(E_{p_b}+m_b)}{(E_{p_b+k}+m_b)}}$$
$$I_c = \sqrt{2M_{B_c^*}2E_k}\int d\vec{p}_c \frac{\mathcal{G}_{B_c^*}(-\vec{p}_c,\vec{p}_c)\mathcal{G}_{B_c}(-\vec{p}_c,\vec{p}_c+\vec{k})}{\sqrt{2E_{p_c}2E_{p_c+k}\bar{N}_{B_c^*}(0)\bar{N}_{B_c}(\vec{k})}}\sqrt{\frac{(E_{p_c}+m_c)}{(E_{p_c+k}+m_c)}} \tag{14}$$

Then the decay width $\Gamma(B_c^*\to B_c e^+e^-)$ calculated from the generic expression,

$$\underline{\Gamma} = \frac{1}{(2\pi)^5}\frac{1}{2M_{B_c^*}}\int\frac{d\vec{k}d\vec{k}_1 d\vec{k}_2}{2E_k 2E_{k_1}2E_{k_2}}\delta^{(4)}(k+k_1+k_2-\hat{O}M_{B_c^*})\bar{\sum}_{S_V,\delta}|\mathcal{M}_{fi}|^2, \tag{15}$$

is obtained in terms of hadronic H_{ij} and leptonic L^{ij} tensor as

$$\Gamma(B_c^*\to B_c e^+e^-) = \frac{4\alpha_{em}^2}{(2\pi)^3}\int d^3k\bar{\sum}_{S_V,\delta}H_{ij}L^{ij} \tag{16}$$

when,

$$L^{ij} = \int \frac{d\vec{k}_1 d\vec{k}_2}{2E_{k_1} 2E_{k_2}} \delta^{(4)}(k + k_1 + k_2 - \hat{O} M_{B_c^*}) \times \mathrm{Tr}[(\not{k}_2 + m_e)\gamma^i(\not{k}_1 - m_e)\gamma^j]/(k_1 + k_2)^4. \quad (17)$$

Here the lepton masses are taken as $m_{e^+} = m_{e^-} = m_e$.

Evaluating trace and adopting standard technique of integration via conversion of the three-momentum integral to the four-momentum integral, L^{ij} is simplified to

$$L^{ij} = \frac{2\pi}{3} \frac{\delta^{ij}}{(M_{B_c^*} - E_k)}. \quad (18)$$

Due to δ^{ij} in the expression for L^{ij}, H_{ij} is reduced to H_{ii}. Note that summing over polarization index and spin states and averaging over B_c^* spin states, one gets $\bar{\sum}_{S_V,\delta} |(\vec{\epsilon} \times \vec{k})_i|^2 = \frac{2}{3}|\vec{k}|^2$ which leads to the contribution of the hadronic tensor H_{ii} in terms of transition form factor $F_{B_c^* B_c}(q^2)$ as

$$\bar{\sum}_{S_V,\delta} H_{ii} = \frac{|\vec{k}|^2}{3} |F_{B_c^* B_c}(q^2)|^2 \quad (19)$$

Now casting the leptonic and hadronic tensor each as function of q^2 and finally integrating out q^2 in the kinematic range: $(2m_e)^2 \le q^2 \le (m_{B_c^*} - m_{B_c})^2$, the decay width is obtained in the form

$$\Gamma(B_c^* \to B_c e^+ e^-) = \frac{2\alpha_{em}^2}{9\pi} \int_{(2m_e)^2}^{(M_{B_c^*} - M_{B_c})^2} dq^2 \frac{E_k (E_k^2 - M_{B_c}^2)^{3/2}}{2M_{B_c^*}(M_{B_c^*} - E_k)^2} |F_{B_c^* B_c}(q^2)|^2 \quad (20)$$

where the energy of B_c is

$$E_k = \frac{M_{B_c^*}^2 - M_{B_c}^2 - q^2}{2M_{B_c^*}}$$

In view of recent progress in experimental probe for possible detection of orbitally exited states of B_c and B_c^*, we also evaluate $V \to P e^+ e^-$ type transitions: $B_c^*(2s) \to B_c(2s) e^+ e^-$, $B_c^*(2s) \to B_c e^+ e^-$; $B_c^*(3s) \to B_c(3s) e^+ e^-$, $B_c^*(3s) \to B_c(2s) e^+ e^-$, $B_c^*(3s) \to B_c e^+ e^-$, and $P \to V e^+ e^-$ type transitions: $B_c(2s) \to B_c^* e^+ e^-$, $B_c(3s) \to B_c^*(2s) e^+ e^-$, $B_c(3s) \to B_c^*(1s) e^+ e^-$. For $P \to V e^+ e^-$ type transitions the form factor $F_{PV}(q^2)$ can be calculated in the RIQ model as is done above for $F_{VP}(q^2)$ describing $B_c^* \to B_c e^+ e^-$ involving ground states of the participating mesons. The corresponding decay width expression can be obtained in the form

$$\Gamma[B_c(ns) \to B_c^*(n's)] = \frac{2\alpha_{em}^2}{3\pi} \int_{(2m_e)^2}^{(M_{B_c(ns)} - M_{B_c^*(n's)})^2} dq^2 \frac{E_k (E_k^2 - M_{B_c^*(n's)}^2)^{3/2}}{2M_{B_c(ns)}(M_{B_c(ns)} - E_k)^2} \times |F_{B_c B_c^*}(q^2)|^2. \quad (21)$$

where $n > n'$. In principle one could extend same analysis to the decay processes involving higher orbital excited states with $n \ge 4$ and P-wave states of the B_c family. But because their production rates are negligibly small and experimental measurements are much more difficult, we do not include those transitions in the present analysis.

III. NUMERICAL RESULTS AND DISCUSSION

For numerical analysis of $B_c^* \to B_c e^+ e^-$ involving B_c^* and B_c meson in their ground states, we take relevant quark masses m_q, corresponding binding energy E_q and potential parameters(a,V_0) which have already been fixed [35] in the RIQ model by fitting the data of heavy flavored mesons including B_c. Using the same set of input parameters, a wide ranging hadronic phenomena [32–42] have been described in earlier applications of this model. Accordingly we take

$$(a, V_0) \equiv (0.017\,166\ \mathrm{GeV}^3, -0.1375\ \mathrm{GeV})$$
$$(m_b, m_c, E_b, E_c) \equiv (4.776\,59, 1.492\,76, 4.766\,33, 1.579\,51)\ \mathrm{GeV} \quad (22)$$

Since $B_c^*(1s)$ has not yet been observed, we take our predicted meson masses; $M_{B_c} = 6.2642$ GeV and $M_{B_c^*} = 6.3078$ GeV [38] obtained through hyperfine mass splitting in the model. Our predicted value of M_{B_c} is close to the central value ~6.2751 GeV of its observed one [44]. However for binding energies of constituent quarks in higher excited states, we solve the cubic equation representing respective bound state condition and obtain

$$(E_b; E_c) = (5.053\,66; 1.970\,16)\ \mathrm{GeV}$$
$$(E_b; E_c) = (5.217\,03; 2.224\,79)\ \mathrm{GeV} \quad (23)$$

for 2 s and 3 s states, respectively. With the quark binding energies (23) and other input parameters as in (22), the mass splitting yields $M_{B_c^*}(2s) = 6.785\,21$ GeV and $M_{B_c^*}(3s) = 6.885\,01$ GeV. The mass of $B_c(2s)$ so predicted runs short of 57 MeV from the observed value of $6842 \pm 4 \pm 5$ MeV [15]. The difficulty encountered here is to make sure all the meson states to have their respective correct masses. This is indeed a problem common to all potential models. Just as in all other model descriptions, we too cannot expect to get precise meson masses for all states with same set of input parameters. So we adjust the potential parameter V_0 to a new value $\sim -0.015\,45$ GeV [34] as is done by T. Wang *et al.* in their work based on the instantaneous approximated Bethe-Salpeter approach [25]. In doing so, we obtain the mass of $B_c(2s)$ equal to its observed value. With

$V_0 = -0.015\,45$ GeV and input parameters (22) and (23), the masses of the B_c, B_c^* meson in 2 s and 3 s states are predicted, respectively, as

$$(M_{B_c^*}(2s); M_{B_c}(2s)) = (6910.3; 6841.9)\ \text{MeV}$$
$$(M_{B_c^*}(3s); M_{B_c}(3s)) = (7259.5; 7135.6)\ \text{MeV}. \quad (24)$$

Using appropriate wave packets for participating mesons in the hadronic part and simplifying the hadronic and leptonic part separately, we calculate the S-matrix element (8)–(11). Then the invariant transition matrix elements $\mathcal{M}_{fi}$ (12)–(14) are calculated from which we finally extract the model expression for transition form factor (19).

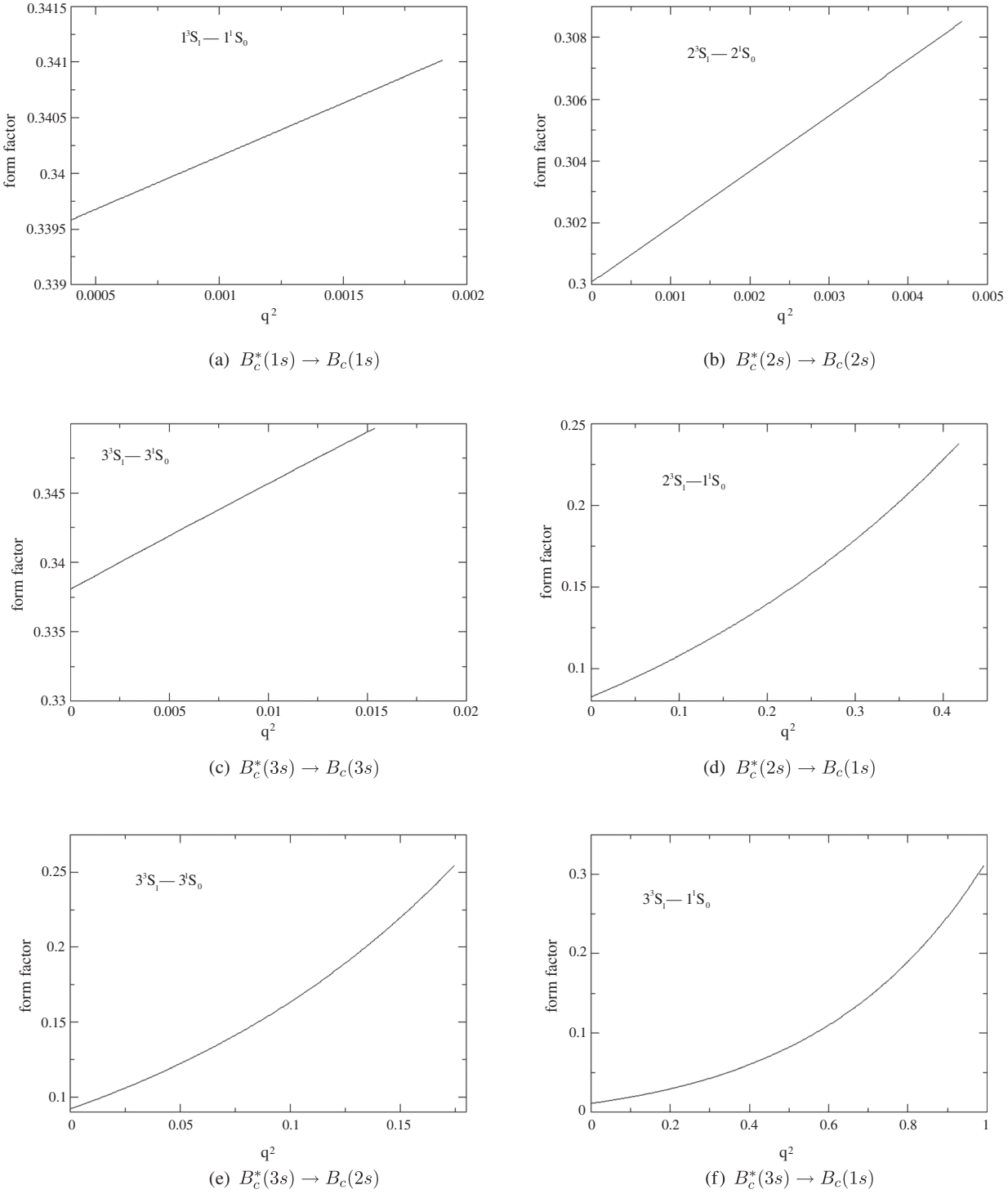

(a) $B_c^*(1s) \to B_c(1s)$ (b) $B_c^*(2s) \to B_c(2s)$

(c) $B_c^*(3s) \to B_c(3s)$ (d) $B_c^*(2s) \to B_c(1s)$

(e) $B_c^*(3s) \to B_c(2s)$ (f) $B_c^*(3s) \to B_c(1s)$

FIG. 2. The q^2 dependence of form factor of $B_c^* \to B_c$.

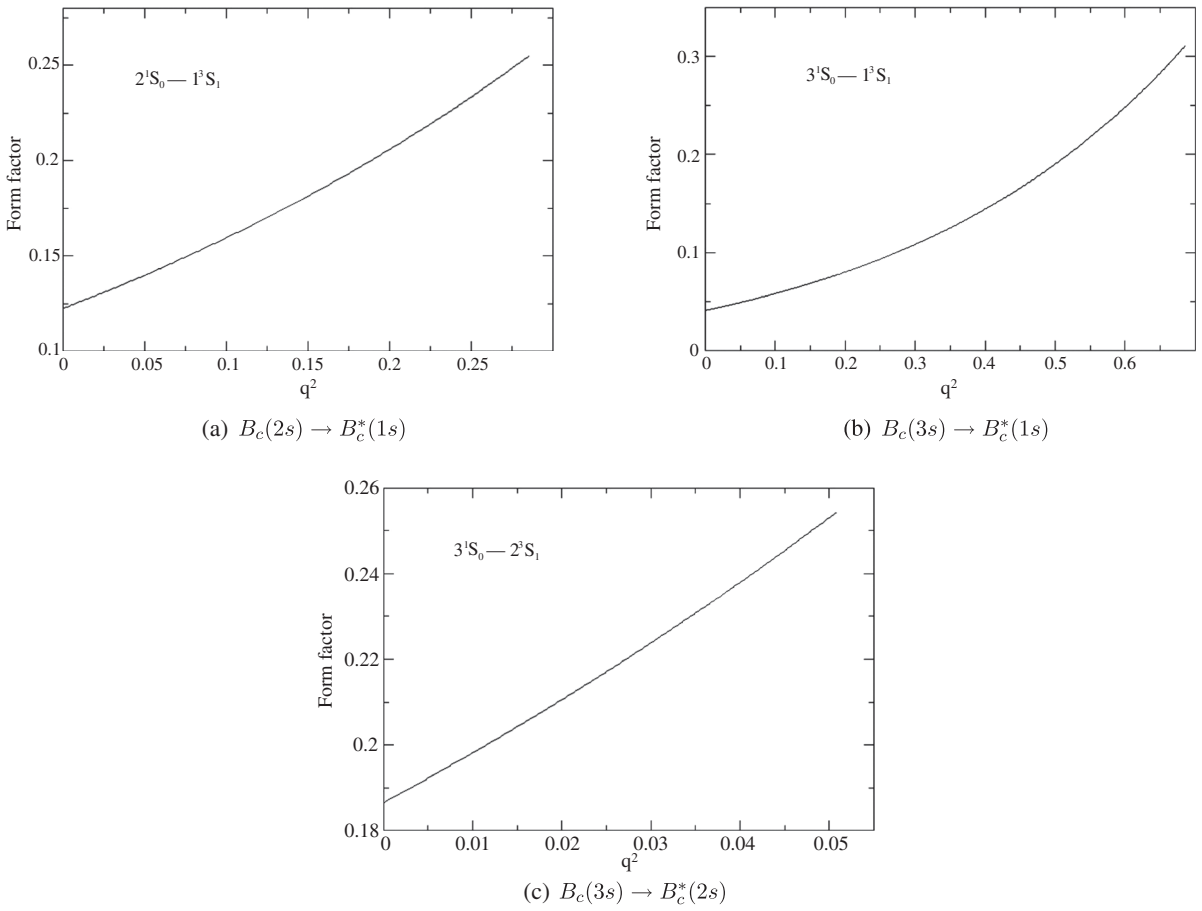

FIG. 3. The q^2 dependence of form factor of $B_c \to B_c^*$.

We then study the q^2 dependence of $F_{B_c^* B_c}(q^2)$ and $F_{B_c B_c^*}(q^2)$ for different decay modes in respective kinematic ranges, which are depicted in Figs. 2 and 3. For transitions $B_c^*(ns) \to B_c(n's)e^+e^-$ where the mass splitting is marginal, the transition form factors are found to increase almost linearly with q^2. In other transitions, $B_c^*(ns) \to B_c(n's)e^+e^-$ and $B_c(ns) \to B_c^*(n's)e^+e^-$ with quantum number $n > n'$, where the mass difference between the participating mesons is comparatively large, the q^2 dependence of the form factors is found to be parabolic. This is contrary to the predictions of the model calculation based on the Bethe-Salpeter framework [17], where the form factors are found to be almost constant in the respective kinematic range for which they consider $F_{B_c^* B_c}(q^2) = F_{B_c^* B_c}(q^2_{\rm min})$ for their calculation accuracy. However, in the present work, we do not resort to such an approximation and instead use the calculated form factors as such with their q^2 dependence in the respective kinematic range to evaluate the decay widths.

Then, substituting the model expressions for $F_{B_c^* B_c}(q^2)$ and $F_{B_c B_c^*}(q^2)$ in Eqs. (20) and (21), respectively, we evaluate the decay widths for transitions involving mesons in 1 s, 2 s, and 3 s states. The predicted decay rates are listed in Table I.

The transitions $B_c^*(ns) \to B_c(ns)e^+e^-$ are known as allowed transitions, whereas $B_c^*(ns) \to B_c(n's)e^+e^-$ and $B_c(ns) \to B_c^*(n's)e^+e^-$ together are known as hindered transitions. In the latter type of transitions, n is greater than n'. In this work, we have analyzed both the allowed and hindered transitions. In the field theoretic description of any decay process, the relativistic effects are implicitly incorporated into the analysis by invoking precise spin-spin interaction while extracting the wave function in the model framework and reproducing hyperfine mass splitting

TABLE I. Comparison of theoretical prediction on decay rates (in keV) for several electromagnetic transitions.

Transitions	Present work	[17]
$1^3S_1 \to 1^1S_0$	0.7112×10^{-5}	8.64×10^{-5}
$2^3S_1 \to 2^1S_0$	0.2168×10^{-4}	⋯
$3^3S_1 \to 3^1S_0$	0.1621×10^{-3}	⋯
$2^3S_1 \to 1^1S_0$	0.2452×10^{-3}	1.59×10^{-3}
$3^3S_1 \to 2^1S_0$	0.0824×10^{-3}	⋯
$3^3S_1 \to 1^1S_0$	2.3569×10^{-3}	2.11×10^{-3}
$2^1S_0 \to 1^3S_1$	0.7297×10^{-3}	1.65×10^{-3}
$3^1S_0 \to 2^3S_1$	0.1035×10^{-3}	1.41×10^{-3}
$3^1S_0 \to 1^3S_1$	9.4391×10^{-3}	0.42×10^{-3}

between the vector mesons and their pseudoscalar counterparts. In the present work, the relativistic recoil effect on the antiquark $\bar{c}$, which is not so heavy compared to the quark b, is found to be significant. This along with the interaction potential $U(r)$, taken in equally mixed scalar-vector harmonic form, yields the results as shown in Table I. On closer scrutiny, we find that between our results and those of [17], there is roughly an order of magnitude difference for all the transitions except in one ($3^3S_1 \to 1^1S_0$). This might be due to the fact that the authors in [17] have approximated the relevant form factors in respective transitions to be a constant, i.e., $F(q^2) \sim F(q^2_{\rm min})$ for their calculation accuracy, although the form factors are expected to vary with q^2 in their allowed kinematic ranges. In fact, the variations of form factors with q^2 in the allowed as well as hindered transitions in their respective kinematic ranges are found here either in linear or parabolic form as shown in Figs. 2 and 3, and accordingly we predicted the decay widths. Thus, we have not taken any kind of approximation at the form factor level. In the absence of any experimental data in this sector, the future experiments would tell which model is suitable to describe these electromagnetic transitions. We hope our predictions in this sector will provide helpful guidance in the experimental studies of reactions with these particles. Fortunately, the experiments at the LHC and Z^0 factory are likely to detect the ground state of B_c^* and other excited states of the B_c meson in the near future.

IV. SUMMARY AND CONCLUSION

We study electromagnetic transitions: $B_c^*(ns) \to B_c(ns)e^+e^-$, $B_c^*(ns) \to B_c(n's)e^+e^-$ and $B_c(ns) \to B_c^*(n's)e^+e^-$ with the quantum number $n > n'$ in the framework of the relativistic independent quark model based on the interaction potential in equally mixed scalar-vector harmonic form. We obtain a model expression of the quark and antiquark momentum probability amplitude $G_b(p_b)$ and $\tilde{G}_c(p_c)$ by taking momentum projections of respective quark orbitals derived in this model after solving Dirac equation. With an effective momentum profile function considered as

$$\mathcal{G}_{B_c}(\vec{p}_b, \vec{p}_{\bar{c}}) = \sqrt{G_b(\vec{p}_b)\tilde{G}_{\bar{c}}(\vec{p}_{\bar{c}})},$$

we construct appropriate wave packets that represent participating meson states at definite momentum and spin and then calculate the transition matrix element from which the transition form factors are extracted. For numerical analysis, we consider input parameters such as quark mass m_q and corresponding binding energy E_q and model parameters (a, V_0) which have already been fixed by fitting with heavy flavor data in order to describe the decay process involving ground states. For determining the mass of B_c and B_c^* in their orbitally excited states (2 s and 3 s), we first calculate the binding energies of constituent quarks by solving cubic equations that represent the bound state condition for respective constituent quarks. Then we fine-tune the potential parameter V_0 to a new value $\sim -0.015\,45$ GeV, while retaining the quark masses and model parameters as those used for 1 s states, and reproduce hyperfine splitting to get a psuedoscalar $B_c(2s)$ mass equal to its observed value. However, for the transitions involving the B_c and B_c^* mesons in 3 s states, we had to take the same set of input parameters as used for the hyperfine splitting of mesons in 2 s states since neither of the $B_c(3s)$ and $B_c^*(3s)$ states have been observed. With these two sets of input parameters—one for transition involving 1 s state and others involving 2 s and 3 s states of B_c and B_c^*, we obtain numerically the transition form factor for each q^2 value in its respective kinematic range.

Then we study the q^2 dependence of the transition form factor $F_{B_c^*B_c}(q^2)$ and $F_{B_cB_c^*}(q^2)$ for energetically possible transitions of the type $V \to Pe^+e^-$ as well as $P \to Ve^+e^-$ involving ground and orbitally excited states (2 s and 3 s states) of the B_c family members. We find that for allowed transitions $B_c^*(ns) \to B_c(ns)e^+e^-$, where the mass splitting is marginal, the transition form factors increase linearly with q^2 in the kinetic range of $(2m_e)^2 \le q^2 \le (m_{B_c^*(ns)} - m_{B_c(ns))})^2$. However, for hindered transitions of the type $V \to Pe^+e^-$: $B_c^*(ns) \to B_c(n's)e^+e^-$ and $P \to Ve^+e^-$: $B_c(ns) \to B_c^*(n's)e^+e^-$ with $n > n'$, where the mass difference between the parent and daughter mesons is comparably large, the q^2 dependence of the relevant transition form factors is found to be parabolic. Our predictions here are contrary to the results obtained in the model calculations based on the Bethe-Salpeter approximation. They find the transition form factor to be almost constant in the entire kinematic range and, hence, consider $F_{B_c^*B_c}(q^2) = F_{B_c^*B_c}(q^2_{\rm min})$ only for their calculation accuracy. We then substitute the model expression for the relevant transition form factor into the decay width expression, and then integrate out q^2 in the respective kinematic range and evaluate the decay widths for the allowed and hindered transitions. In the RIQ model formalism, the relativistic effect is incorporated into the analysis by invoking precise spin-spin interaction, while extracting the wave function and reproducing mass splitting between the vector meson and its pseudoscalar counterpart. On scrutiny, we find that the relativistic recoil on the antiquark $\bar{c}$, which is not so heavy compared to the heavy quark b, is found to be more significant. This, along with our choice of interaction potential in equally mixed scalar-vector harmonic form, leads to our predicted decay widths for energetically possible transitions as shown in Table I. Our predictions in this sector are compared with those obtained in the model calculation based on the Bethe-Salpeter approach [17]. On closer scrutiny, we find that between our results and those of [17], there is roughly an order of magnitude

difference for all the transitions except in one ($3^3S_1 \to 1^1S_0$). This might be due to the fact that the authors in [17] have approximated the relevant form factors in respective transitions to be a constant, i.e., $F(q^2) \sim F(q^2_{\rm min})$ for their calculation accuracy, although the form factors are expected to vary with q^2 in their allowed kinematic ranges. In fact, the variations of form factors with q^2 in the allowed as well as hindered transitions in their respective kinematic ranges are found here either in linear or parabolic form as shown in Figs. 2 and 3 and accordingly we predicted the decay widths. Thus we have not taken any kind of approximation at the form factor level. In the absence of precise data in this sector only the future experiments at LHC and Z^0-factory would tell which model is more suitable to provides realistic description of these transitions. Fortunately the experiments at LHCb and particularly Z^0-factory are likely to provide precise data in the near future.

ACKNOWLEDGMENTS

S. Patnaik acknowledges the library and computational facilities provided by the authorities of Siksha 'O' Anusandhan Deemed to be University, Bhubaneswar 751 030, India, to carry out the present work.

APPENDIX: CONSTITUENT QUARK ORBITALS AND MOMENTUM PROBABILITY AMPLITUDES

In the RIQ model, a meson is pictured as a color-singlet assembly of a quark and an antiquark independently confined by an effective and average flavor independent potential in the form: $U(r) = \frac{1}{2}(1+\gamma^0)(ar^2 + V_0)$ where (a, V_0) are the potential parameters. It is believed that the zeroth-order quark dynamics generated by the phenomological confining potential $U(r)$ taken in equally mixed scalar-vector harmonic form can provide adequate tree level description of the decay process being analyzed in this work. With the interaction potential $U(r)$ put into the zeroth-order quark Lagrangian density, the ensuing Dirac equation admits static solution of positive and negative energy as:

$$\psi^{(+)}_{\xi}(\vec{r}) = \begin{pmatrix} \frac{ig_{\xi}(r)}{r} \\ \frac{\vec{\sigma}.\hat{r} f_{\xi}(r)}{r} \end{pmatrix} U_{\xi}(\hat{r})$$
$$\psi^{(-)}_{\xi}(\vec{r}) = \begin{pmatrix} \frac{i(\vec{\sigma}.\hat{r}) f_{\xi}(r)}{r} \\ \frac{g_{\xi}(r)}{r} \end{pmatrix} \tilde{U}_{\xi}(\hat{r}) \tag{A1}$$

where, $\xi = (nlj)$ represents a set of Dirac quantum numbers specifying the eigen-modes; $U_{\xi}(\hat{r})$ and $\tilde{U}_{\xi}(\hat{r})$ are the spin angular parts given by,

$$U_{ljm}(\hat{r}) = \sum_{m_l, m_s} \langle l m_l \frac{1}{2} m_s | jm \rangle Y^{m_l}_{l}(\hat{r}) \chi^{m_s}_{\frac{1}{2}}$$
$$\tilde{U}_{ljm}(\hat{r}) = (-1)^{j+m-l} U_{lj-m}(\hat{r}) \tag{A2}$$

With the quark binding energy E_q and quark mass m_q written in the form $E'_q = (E_q - V_0/2)$, $m'_q = (m_q + V_0/2)$ and $\omega_q = E'_q + m'_q$, one can obtain solutions to the resulting radial equation for $g_{\xi}(r)$ and $f_{\xi}(r)$ in the form

$$g_{nl} = N_{nl}\left(\frac{r}{r_{nl}}\right)^{l+l} \exp(-r^2/2r^2_{nl}) L^{l+1/2}_{n-1}(r^2/r^2_{nl})$$
$$f_{nl} = N_{nl}\left(\frac{r}{r_{nl}}\right)^{l} \exp(-r^2/2r^2_{nl}) \times \left[\left(n + l - \frac{1}{2}\right) L^{l-1/2}_{n-1}(r^2/r^2_{nl}) + n L^{l-1/2}_{n}(r^2/r^2_{nl})\right], \tag{A3}$$

where, $r_{nl} = a\omega_q^{-1/4}$ is a state independent length parameter, N_{nl} is an overall normalization constant given by

$$N^2_{nl} = \frac{4\Gamma(n)}{\Gamma(n+l+1/2)} \frac{(\omega_{nl}/r_{nl})}{(3E'_q + m'_q)} \tag{A4}$$

and $L^{l+1/2}_{n-1}(r^2/r^2_{nl})$ etc. are associated Laguerre polynomials. The radial solutions yield an independent quark bound-state condition in the form of a cubic equation:

$$\sqrt{(\omega_q/a)}(E'_q - m'_q) = (4n + 2l - 1). \tag{A5}$$

The solution of the cubic equation provides the zeroth-order binding energies of the confined quark and antiquark for all possible eigenmodes.

In the relativistic independent particle picture of this model, the constituent quark and antiquark are thought to move independently inside the B_c-meson bound state with momentum $\vec{p}_b$ and $\vec{p}_c$, respectively. Their individual momentum probability amplitudes are obtained in this model via momentum projection of the respective quark orbitals (A1) in the following forms: For the ground state mesons ($n = 1$, $l = 0$):

$$G_b(\vec{p}_b) = \frac{i\pi\mathcal{N}_b}{2\alpha_b\omega_b}\sqrt{\frac{(E_{p_b} + m_b)}{E_{p_b}}}(E_{p_b} + E_b)\exp\left(-\frac{\vec{p}^2}{4\alpha_b}\right)$$
$$\tilde{G}_c(\vec{p}_c) = -\frac{i\pi\mathcal{N}_c}{2\alpha_c\omega_c}\sqrt{\frac{(E_{p_c} + m_c)}{E_{p_c}}}(E_{p_c} + E_c)\exp\left(-\frac{\vec{p}^2}{4\alpha_c}\right). \tag{A6}$$

For the excited meson state ($n = 2$, $l = 0$):

$$G_b(\vec{p}_b) = \frac{i\pi\mathcal{N}_b}{2\alpha_b\omega_b}\sqrt{\frac{(E_{p_b}+m_b)}{E_{p_b}}}\exp\left(-\frac{\vec{p}^2}{4\alpha_b}\right)\sqrt{(A_b^2+B_b^2)}e^{i\phi_b}$$
$$\tilde{G}_c(\vec{p}_c) = -\frac{i\pi\mathcal{N}_c}{2\alpha_c\omega_c}\sqrt{\frac{(E_{p_c}+m_c)}{E_{p_c}}}\exp\left(-\frac{\vec{p}^2}{4\alpha_c}\right)\sqrt{(A_c^2+B_c^2)}e^{i\phi_c}, \tag{A7}$$

where

$$A_{b,c} = \frac{3}{\sqrt{\pi}}(E_{p_{b,c}}-m_{b,c})\sqrt{\frac{\alpha_{b,c}}{p_{b,c}^2}}\left(3-\frac{p_{b,c}^2}{\alpha_{b,c}}\right)$$
$$B_{b,c} = \frac{\omega_{b,c}}{2}\left(\frac{p_{b,c}^2}{\alpha_{b,c}}-3\right)+(E_{p_{b,c}}-m_{b,c})\left(1+\frac{\alpha_{b,c}}{p_{b,c}^2}\right). \tag{A8}$$

For the excited meson state ($n=3$, $l=0$):

$$G_b(\vec{p}_b) = \frac{i\pi\mathcal{N}_b}{4\alpha_b\omega_b}\sqrt{\frac{(E_{p_b}+m_b)}{E_{p_b}}}\exp\left(-\frac{\vec{p}^2}{4\alpha_b}\right)\sqrt{(A_b^2+B_b^2)}e^{i\phi_b}$$
$$\tilde{G}_c(\vec{p}_c) = -\frac{i\pi\mathcal{N}_c}{4\alpha_c\omega_c}\sqrt{\frac{(E_{p_c}+m_c)}{E_{p_c}}}\exp\left(-\frac{\vec{p}^2}{4\alpha_c}\right)\sqrt{(A_c^2+B_c^2)}e^{i\phi_c}, \tag{A9}$$

where

$$A_{b,c} = \frac{\omega_{b,c}}{2p_{b,c}}\sqrt{\frac{\alpha_{b,c}}{\pi}}\left(\frac{5p_{b,c}^4}{\alpha_{bc}^2}-26\frac{p_{b,c}^2}{\alpha_{b,c}}-41\right)$$
$$B_{b,c} = \omega_{b,c}\left(\frac{p_{b,c}^4}{4\alpha_{b,c}^2}-\frac{5p_{b,c}^2}{2\alpha_{b,c}}+\frac{15}{4}\right)+(E_{p_{b,c}}-m_{b,c})\frac{\alpha_{b,c}}{2p_{b,c}^2}\left(\frac{p_{b,c}^4}{\alpha_{b,c}^2}-\frac{2p_{b,c}^2}{\alpha_{b,c}}+7\right). \tag{A10}$$

For both the 2 s and 3 s states,

$$\phi_{b,c} = \tan^{-1}\frac{B_{b,c}}{A_{b,c}}$$

with their respective $A_{b,c}$ and $B_{b,c}$.

The binding energies of the constituent quark and antiquark for ground and orbitally excited B_c and B_c^* states can also be obtained by solving respective cubic equations with $n=1, 2, 3$ and $l=0$ representing appropriate bound-state conditions by putting the quantum number $n=1, 2, 3$ and $l=0$.

[1] F. Abe *et al.* (CDF Collaboration), Phys. Rev. D **58**, 112004 (1998).
[2] C. H. Chang and Y. Q. Chen, Phys. Lett. B **284**, 127 (1992).
[3] C. H. Chang and Y. Q. Chen, Phys. Rev. D **46**, 3845 (1992); **50**, 6013(E) (1994).
[4] C. H. Chang and Y. Q. Chen, Phys. Rev. D **48**, 4086 (1993).
[5] R. Barate (ALEPH Collaboration), Phys. Lett. B **402**, 213 (1997).
[6] P. Abreu (DELPHI Collaboration) Phys. Lett. B **398**, 207 (1997).
[7] K. Acker (OPAL Collaboration), Phys. Lett. B **420**, 157 (1998).
[8] K. Cheung, Phys. Lett. B **472**, 408 (2000).
[9] W. C. Wester (CDF and D0 Collaborations) Nucl. Phys. B, Proc. Suppl. **156**, 240 (2006).
[10] A. Abulencia *et al.*, Phys. Rev. Lett. **97**, 012002 (2006).

[11] V. M. Abazov *et al.*, Phys. Rev. Lett. **102**, 092001 (2009).
[12] T. A. Aaltonen *et al.*, Phys. Rev. Lett. **100**, 182002 (2008).
[13] V. M. Abazov *et al.*, Phys. Rev. Lett. **101**, 012001 (2008).
[14] R. Aajj *et al.* (LHCb Collaboration), Eur. Phys. J. C **74**, 2839 (2014).
[15] G. Aad *et al.* (ATLAS Collaboration), Phys. Rev. Lett. **113**, 212004 (2014).
[16] H. W. Ke and X. Q. Li, Sci. China Phys. Mech. Astron. **53**, 2019 (2010).
[17] K. E. Hong Wei, G. L. Wang, X. Q. Li, and C. H. Chang, Sci. China **53**, 2025 (2010).
[18] E. J. Eichten and C. Quigg, Phys. Rev. D **49**, 5845 (1994).
[19] S. S. Gershtein, V. V. Kiselev, A. K. Lakhoded, and A. V. Tkabladze, Phys. Usp. **38**, 1 (1995); Phys. Rev. D **51**, 3613 (1995); E. O. Iltan, J. Phys. G **27**, 1723 (2001).
[20] S. N. Gupta and J. M. Johnson, Phys. Rev. D **53**, 312 (1996).
[21] L. P. Fulcher, Phys. Rev. D **60**, 074006 (1999).
[22] D. Ebert, R. N. Faustov, and V. O. Galkin, Phys. Rev. D **67**, 014027 (2003).
[23] S. Godfrey, Phys. Rev. D **70**, 054017 (2004); S. Godfrey and N. Isgur, Phys. Rev. D **32**, 189 (1985).
[24] A. Abd. El-Hady *et al.*, Phys. Rev. D **71**, 034006 (2005).
[25] T. Wang, Y. Jiang, W.-L. Ju, and H. Yuan, J. High Energy Phys. 03 (2016) 209.
[26] E. E. Salpeter and H. A. Bethe, Phys. Rev. **84**, 1232 (1951).
[27] N. Brambilla *et al.*, Eur. Phys. J. C **71**, 1534 (2011); N. Devlani, V. Kher, and A. K. Rai, Eur. Phys. J. A **50**, 154 (2014).
[28] T. M. Aliev, E. Iltan, and N. K. Pak, Phys. Lett. B **329**, 123 (1994).
[29] H.-M. Choi and C.-R. Ji, Phys. Rev. D **80**, 054016 (2009).
[30] Z.-G. Wang, Eur. Phys. J. C **73**, 2559 (2013).
[31] D. Becirevie and B. Hass, Eur. Phys. J. C **71**, 1734 (2011); A. Abada, D. Becirevic, Ph. Boucaud, G. Herdoiza, J. P. Leroy, A. Le Yaouanc, O. Pene, and J. Rodriguez-Quintero, Phys. Rev. D **66**, 074504 (2002).
[32] N. Barik, P. C. Dash, and A. R. Panda, Phys. Rev. D **46**, 3856 (1992); N. Barik and P. C. Dash, Phys. Rev. D **49**, 299 (1994).
[33] M. Priyadarsini, P. C. Dash, S. Kar, S. P. Patra, and N. Barik, Phys. Rev. D **94**, 113011 (2016).
[34] S. Patnaik, P. C. Dash, S. Kar, S. P. Patra, and N. Barik, Phys. Rev. D **96**, 116010 (2017).
[35] N. Barik and B. K. Dash, Phys. Rev. D **33**, 1925 (1986); N. Barik, B. K. Dash, and P. C. Dash, Pramana **29**, 543 (1987); N. Barik and P. C. Dash, Phys. Rev. D **47**, 2788 (1993).
[36] M. Priyadarsini, P. C. Dash, S. Kar, S. P. Patra, and N. Barik, Phys. Rev. D **94**, 113011 (2016); N. Barik and P. C. Dash, Mod. Phys. Lett. A **10**, 103 (1995); N. Barik, S. Kar, and P. C. Dash, Phys. Rev. D **57**, 405 (1998); N. Barik, Sk. Naimuddin, S. Kar, and P. C. Dash, Phys. Rev. D **63**, 014024 (2000).
[37] N. Barik, P. C. Dash, and A. R. Panda, Phys. Rev. D **47**, 1001 (1993).
[38] N. Barik and P. C. Dash, Phys. Rev. D **47**, 2788 (1993).
[39] N. Barik, Sk. Naimuddin, P. C. Dash, and S. Kar, Phys. Rev. D **77**, 014038 (2008); **78**, 114030 (2008); N. Barik, Sk. Naimuddin, and P. C. Dash, Mod. Phys. A **24**, 2335 (2009).
[40] N. Barik and P. C. Dash, Phys. Rev. D **53**, 1366 (1996); N. Barik, S. K. Tripathy, S. Kar, and P. C. Dash, Phys. Rev. D **56**, 4238 (1997); N. Barik, Sk. Naimuddin, P. C. Dash, and S. Kar, Phys. Rev. D **80**, 074005 (2009).
[41] N. Barik, S. Kar, and P. C. Dash, Phys. Rev. D **63**, 114002 (2001); S. Kar, P. C. Dash, M. Priyadarsini, Sk. Naimuddin, and N. Barik, Phys. Rev. D **88**, 094014 (2013).
[42] N. Barik, Sk. Naimuddin, P. C. Dash, and S. Kar, Phys. Rev. D **80**, 014004 (2009); Sk. Naimuddin, S. Kar, M. Priyadarsini, N. Barik, and P. C. Dash, Phys. Rev. D **86**, 094028 (2012).
[43] B. Margolis and R. R. Mendel, Phys. Rev. D **28**, 468 (1983).
[44] C. Patrignani *et al.* (Particle Data Group), Chin. Phys. C **40**, 100001 (2016).